Temperature-dependent photoluminescence and carrier dynamics of standard and coupled type-II GaSb/GaAs quantum rings

Wei-Hsun Lin [a], Kai-Wei Wang [b], Shih-Yen Lin [c,d,e,*], Meng-Chyi Wu [a]

[a] Institute of Electronics Engineering, National Tsing Hua University, Hsinchu 300, Taiwan
[b] College of Photonics, National Chiao-Tung University, Tainan 711, Taiwan
[c] Research Center for Applied Sciences, Academia Sinica, Taipei 11529, Taiwan
[d] Department of Photonics, National Chiao-Tung University, Hsinchu 300, Taiwan
[e] Institute of Optoelectronic Sciences, National Taiwan Ocean University, Keelung 20224, Taiwan

ARTICLE INFO

ABSTRACT

Temperature-dependent photoluminescence (PL) and the corresponding carrier dynamics of standard and coupled type-II GaSb/GaAs quantum rings (QRs) are investigated in this article. Compared with standard QRs, the slower PL intensity decay of coupled QRs with increasing temperature is attributed to the depression of thermal quenching. More intense PL intensity is also observed for the coupled-QR sample at room temperature. With further reducing the GaAs spacer layer thickness to 2 nm, near two-times PL enhancement is observed. The results indicate that with the enhanced luminescence intensity of coupled-QR structure, type-II nano-structures may be utilized for light-emitting device applications.

1. Introduction

For decades, quantum dots (QDs) with type-II band alignment have attracted much attention for scientists around the world. The studies on its unique optical characteristics and different applications have been reported in literatures [1–9]. Different from type-I QDs, electrons and holes are separately confined in the type-II QDs. This suggests that if holes or electrons are confined in the type-II QDs, electron or hole shells would loosely surround the QDs due to the Columb interaction [10]. This feature results in the long carrier life time and thus low recombination probability of type-II nano-structures. In this case, it is generally recognized that type-II nano-structures are not suitable for the applications of light-emitting devices. If one would like to use the unique characteristics of the type-II nano-structures for light-emitting devices, the luminescence intensity has to be enhanced. For GaAsSb-capped InAs/GaAs QD structure, it has been demonstrated that well controlling the thickness of GaAsSb in this structure can both obtain long carrier life time and good photoluminescence (PL) intensity [11]. In our recent research, we have also demonstrated that enhanced PL intensity can be obtained by reducing the separation layer of two individually GaSb/GaAs quantum-ring (QR) structures to form a coupled-ring system [12].

The long carrier recombination lifetime is still maintained in this structure. It is attributed to the lower escaping probability of electrons away from the GaAs/GaSb interfaces. However, the temperature-dependent behavior of the structure has not yet been investigated. In this article, temperature-dependent PL and the corresponding carrier dynamics of standard and coupled type-II GaSb/GaAs QRs are investigated. Compared with the standard QRs, the slower PL intensity decay with increasing temperature is observed for the coupled-QR sample. With further reducing the GaAs spacer layer thickness to 2 nm, near two-times PL enhancement is observed.

2. Experiments

The samples investigated in this study were grown on (100)-orientated semi-insulated GaAs substrates by using Riber compact-21 solid source molecular beam epitaxy (MBE) system. In this system, both As and Sb effusion cells adopt valved crackers to control the amounts of As and Sb flux. Two samples with three-period GaSb/GaAs QR embedded in GaAs barrier layers were prepared, which are referred as samples A and B. For sample A, it is a standard GaSb QR sample with 50 nm GaAs separation layers between each GaSb QR layer. For sample B, it is a coupled-QR GaSb sample with 5 nm GaAs separation layers between each GaSb QR layer. The detailed sample structures are listed in Table 1. To obtain the whole GaSb QR morphology, well controlled Sb and background As ratios were adopted during the post Sb soaking procedure. The growth rate of GaSb QD is 0.075ML

* Correspondence to: Research Center for Applied Sciences, Academia Sinica, 128 Sec. 2, Academia Rd., Nankang, Taipei 11529, Taiwan. Tel.: +886 3 574 4364; fax: +886 3 574 5233.
E-mail address: shihyen@gate.sinica.edu.tw (S.-Y. Lin).

per second and the Sb/background As ratio is 0.23 while the Sb beam-equivalent flux pressure (BEP) is 1.4×10^{-7} Torr. The detail growth procedure of the GaSb QRs is discussed elsewhere [11,12]. The $1 \times 1\ \mu m^2$ image observed by atomic-force microscopy (AFM) of sample A is shown in Fig. 1. As shown in this figure, full ring morphology is observed. The average ring height, diameter and density are 1.4, 46.7 nm and $2.32 \times 10^{10}\ cm^{-2}$, respectively. The PL measurement was performed by using the Jobin Yvon's NanoLog3 system coupled with He–Ne laser and a Janis compact optical system.

3. Results and discussion

The temperature-varying PL spectra of samples A and B from 10 to 300 K at a pumping intensity of 0.5 W/cm^2 are shown in Fig. 2(a). Two PL peaks are observed for both samples A and B. To verify the transition pathways of the two peaks, power-varying PL measurements are performed on the two samples. Fig. 2(b) shows the 10 K PL peak energy as a function of the cubic root of power density of excitation power for the two samples. The linear dependence of the PL peak energy with the cubic root of laser pumping power density is observed for both the two peaks of samples A and B. According to this result, the PL peaks should all be resulted from type-II transitions [13]. However, with increasing temperature, the higher-energy PL peak drops faster as compared with the lower-energy PL peak for both the two samples. When the temperature rises beyond 110 K, there would be only one

Table 1
Wafer structures of samples A and B.

Sample	A	B	
3.0 ML GaSb/GaAs QR			
40 nm GaAs			
	10 nm GaAs	3.0 ML GaSb QRs	
		5 nm GaAs	
	3.0 ML GaSb QRs	3.0 ML GaSb QRs	3x
200 nm undoped GaAs			
350 μm GaAs S–I substrate (001)			

Fig. 1. The $1 \times 1\ \mu m^2$ image observed by atomic-force microscopy (AFM) of sample A.

dominant peak appeared for the two samples, which is attributed to the luminescence from the GaSb QRs. In this case, compared with the QR luminescence, the higher-energy PL peaks of two samples should be resulted from the recombination mechanism of the faster increase of electron escaping probability away from the interfaces at higher temperatures. Therefore, we would attribute the lower-energy peak as the transition from the electrons to the localized holes of GaSb QRs while the higher-energy peak as the transition from the electrons to the localized holes of GaSb wetting layers. The fitted activation energy by using the Arrhenius equation is adopted to verify this attribution [14]. Also observed in Fig. 2(a) is the similar PL intensities of QR and WL signals at 10 K. For the coupled QR structure, the improved electron confinement will induce higher electron density accumulated in the GaAs spacer layer. The electrons would equally contribute to optical recombination with holes in the underneath QRs and the above WL, which will result in similar PL intensities of QR and WL signals of Sample B at 10 K.

The integrated PL intensities of QR and WL transitions of samples A and B under different temperatures are shown in Fig. 3. According to the fitting results, the activation energy of QR peaks of samples A and B is nearly the same as ~300 meV. The activation energy of WL peaks for samples A and B is also nearly the same as ~50 meV. Therefore, it proves that the lower- and higher-energy PL peaks are resulted from the electron-hole recombination of the QR and WL structures, respectively. Similar results have also been observed in previous literatures [14,15]. However, compared to the QR integrated PL intensity of sample A, the QR PL intensity of sample B drops slowly at high temperatures. Because of the similar activation energy for both the two transitions, it suggests that the thermal escape of holes from QRs is not the main mechanism responsible for the faster PL intensity decay of sample A at high temperatures. For the standard QR structure as sample A, the electrons just loosely surround the localized holes in the GaSb QRs. Therefore, with increasing the temperature, the electron suffers the lattice vibration and gains the energy to overcome the Coulomb force and would easily escape away from the GaAs/GaSb interfaces. In this case, faster PL intensity drop is observed for sample A at higher temperatures. On the contrary, for the coupled-QR GaSb as sample B, the reduced separation layer between the two GaSb QR layers will suppress the electron escaped rate at high temperatures. In this case, the coupled-QR structure GaSb will depress the thermal quenching effect of type-II GaSb nanostructure.

The temperature-varying full width at half maximum (FWHM) of QR PL peak of samples A and B is shown in Fig. 4. In this figure, the FWHM of QR PL peak of sample A keeps at ~75 meV and dramatically increases to ~100 meV for the temperatures below and above 150 K. It indicates that due to the large valence-band offset of GaSb QRs, it is difficult for localized holes to be redistributed to the adjacent QRs via thermal activation below 150 K. So, the FWHM of the PL peaks would keep in the same range. For temperatures above 150 K, the interactions between the loosely confined electrons and phonons would induce the dramatic increase of FWHM, as observed for sample A. For sample B, the PL FWHM continually drops from 92 to 86 meV in the temperature range of 10–170 K. For the temperatures above 170 K, slow increase of PL FWHM is observed for the sample B. The results suggest that the localized holes in the coupled QR structure may hop vertically to the nearby QRs due to thermal activation. In this case, the holes would redistribute and accumulate in larger QRs. The hole redistribution at low temperatures would depress the FWHM broadening effect resulted from QR size non-uniformity, which would lead to the decrease of PL FWHM of QR of sample B in the temperature range of 10–170 K. For temperatures above 170 K, as the sample A, the same
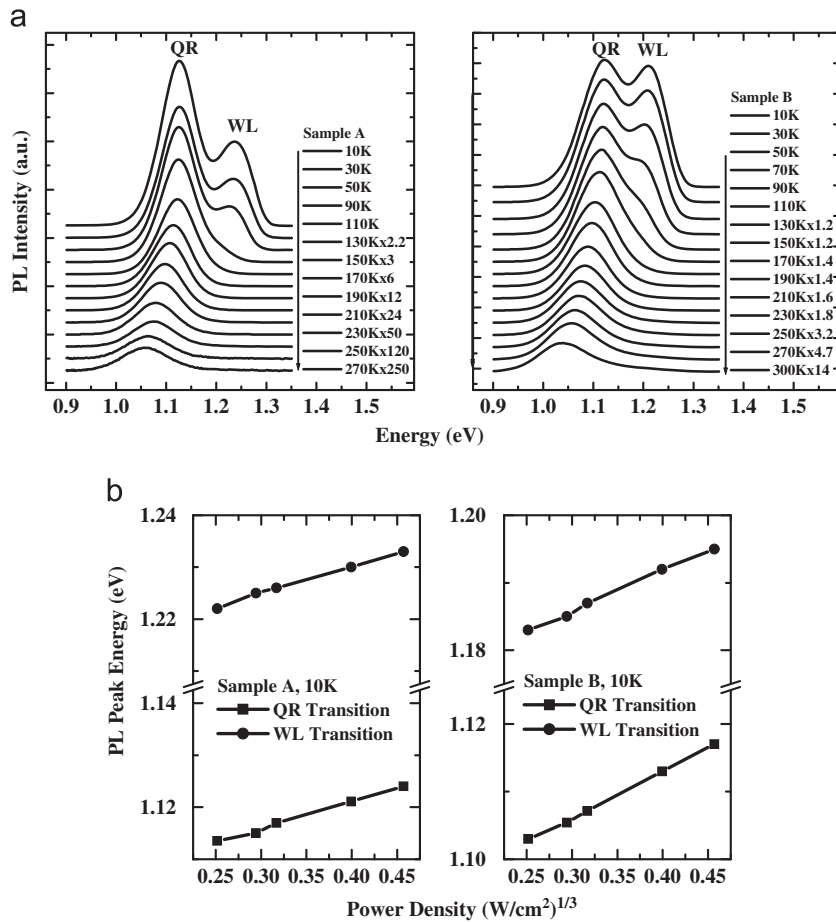
Fig. 2. (a) Temperature-varying PL spectra of samples A and B from 10 to 300 K at a pumping intensity of 0.5 W/cm^2 and (b) the 10 K PL peak energy as a function of the cubic root of power density of excitation power for the two samples.
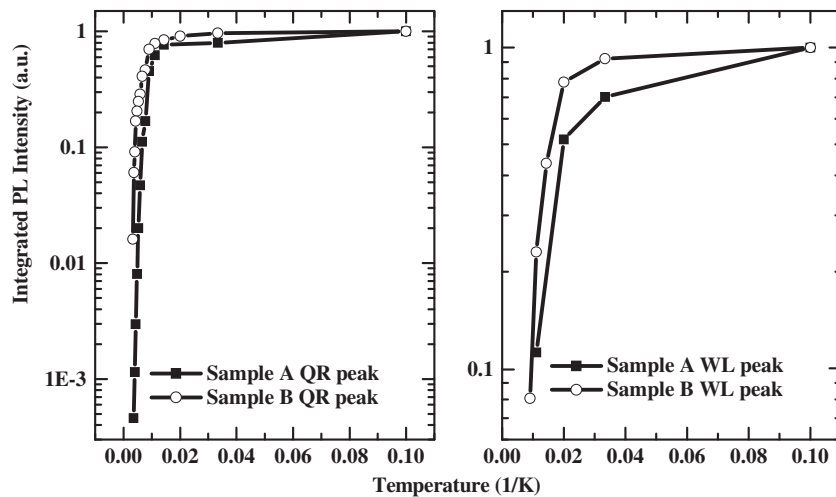

Fig. 3. Integrated PL intensity of QR and WL transitions of samples A and B under different temperatures.

electron–phonon interaction would result in the FWHM broadening for sample B. However, since the tensile-strained GaAs spacer layer between the two GaSb QR layers provides a better confinement for electrons [12], the FWHM broadening of sample B at high temperatures is less significant, as sample A.

Since the coupled-QR structure would exhibit more intense luminescence intensity than the standard QRs at room temperature, it is possible that by further reducing the GaAs spacer layer thickness, more intense PL intensity can be observed. To verify

this assumption, the other coupled-ring sample with a thinner GaAs spacer layer (2 nm) is prepared, which is referred as sample C. Since the ring height is 1.4 nm, the 2 nm GaAs spacer layer is still sufficient to fully cover the GaSb QRs. The room-temperature PL spectra of samples B and C are shown in Fig. 5. An inspection of this figure reveals that two-times stronger PL intensity of sample C than that of sample B is observed. Also observed are the similar spectral shapes of the two samples. The results suggest that the reduced GaAs spacer layer thickness will further enhance the
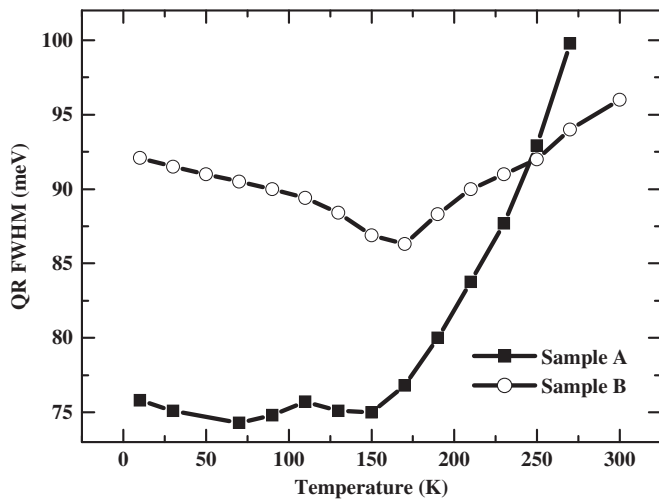
Fig. 4. Temperature-dependent full width at half maximum (FWHM) of QR PL peak of samples A and B.
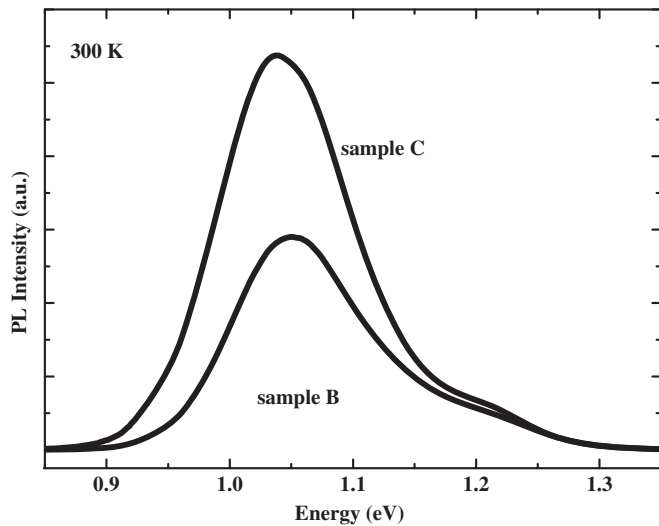

Fig. 5. Room-temperature PL spectra of samples B and C.

luminescence intensity of coupled-QR structures. However, it seems that no significant difference in the QR confinement states is observed even when the spacer layer is reduced to 2 nm. Also observed for Sample C is the similar temperature 170 K when minimum PL peak FWHM is observed. Assuming the hole hopping process does take place in the coupled QR structure, the minimum PL FWHM should be observed at a lower temperature due to the reduced barrier of Sample C. However, since more electrons are accumulated in the GaAs spacer layer of Sample C, the holes would have probability to recombine with the electrons and emit light instead of redistributing to lower hole states in the other QR layer. Therefore, the effects of reducing barrier for hole hopping and increasing recombination probability of Sample C with 2 nm GaAs spacer layer may cancel out with each other such that

similar temperatures are observed for Samples B and C for minimum PL FWHMs. To confirm this attribution, further investigation is still required in the future.

4. Conclusions

In conclusion, temperature-varying PL and the corresponding carrier dynamics of standard and coupled quantum rings (QRs) of type-II GaSb/GaAs are investigated. Slower PL intensity decay is observed for the coupled-QR sample. An increase of the temperature would firstly decrease and then increase the FWHM of QR PL peak. A model is established to explain these phenomena. With a thinner GaAs spacer layer of 2 nm thickness, near two-times PL enhancement is observed. The results exhibit that while maintaining the long carrier lifetime of GaSb QRs, enhanced luminescence intensity can still be obtained for type-II heterostructures by providing better electron confinement. The demonstration of intense luminescence of the type-II coupled-QR structure is advantageous for their application in optical devices with the unique characteristics.

Acknowledgment

References

[1] K. Akahane, N. Yamamoto, N. Ohtani, Physica E 21 (2004) 295.
[2] F. Hatami, N.N. Ledentsov, M. Grundmann, J. Böhrer, F. Heinrichsdorff, M. Beer, D. Bimberg, S.S. Ruvimov, P. Werner, U. Gösele, J. Heydenreich, U. Richter, S.V. Ivanov, B.Ya. Meltser, P.S. Kop'ev, I. Alferov, Applied Physics Letters 67 (1995) 656.
[3] S. Kim, B. Fisher, H. Eisler, M. Bawendi, Journal of the American Chemical Society 125 (2003) 11466.
[4] Y.D. Jang, T.J. Badcock, D.J. Mowbray, M.S. Skolnick, J. Park, D. Lee, H.Y. Liu, M.J. Steer, M. Hopkinson, Applied Physics Letters 92 (2008) 251905.
[5] C.K. Sun, G. Wang, J.E. Bowers, B. Brar, H.R. Blank, H. Kroemer, M.H. Pilkuhn, Applied Physics Letters 68 (1996) 1543.
[6] S. Kim, Y.T. Lim, E.G. Soltesz, A.M. De Grand, J. Lee, A. Nakayama, J.A. Parker, T. Mihaljevic, R.G. Laurence, D.M. Dor, L.H. Cohn, M.G. Bawendi, J.V. Frangioni, Nature Biotechnology 22 (2004) 93.
[7] A. Marent, M. Geller, A. Schliwa, D. Feise, K. Pötschke, D. Bimberg, N. Akçay, N. Öncan, Applied Physics Letters 91 (2007) 242109.
[8] J. Tatebayashi, A. Khoshakhlagh, S.H. Huang, G. Balakrishnan, L.R. Dawson, D.L. Huffaker, D.A. Bussian, H. Htoon, V. Klimov, Applied Physics Letters 90 (2007) 261115.
[9] S.Y. Lin, C.C. Tseng, W.H. Lin, S.C. Mai, S.Y. Wu, S.H. Chen, J.I. Chyi, Applied Physics Letters 96 (2010) 123503.
[10] K. Gradkowski, T.J. Ochalski, N. Pavarelli, H.Y. Liu, J. Tatebayashi, D.P. Williams, D.J. Mowbray, G. Huyet, D.L. Huffaker, Physical Review B 85 (2012) 035432.
[11] W.H. Lin, K.W. Wang, S.W. Chang, M.H. Shih, S.Y. Lin, Applied Physics Letters 101 (2012) 031906.
[12] W.H. Lin, M.Y. Lin, S.Y. Wu, S.Y. Lin, IEEE Photonics Technology Letters 24 (2012) 1203.
[13] D. Alonso-Álvarez, B. Alén, J.M. García, J.M. Ripalda, Applied Physics Letters 91 (2007) 263103.
[14] C. Jiang, H. Sakaki, Physica E 26 (2005) 180.
[15] M. Geller, C. Kapteyn, L. Müller-Kirsch, R. Heitz, D. Bimberg, Applied Physics Letters 82 (2003) 2706.